Unassisted Solar Syngas Production by a Molecular Dye-Cobalt Catalyst Assembly in a Tandem Photoelectrochemical Cell

Duc N. Nguyen, Emmanouil Giannoudis, Tatiana Straistari, Jennifer Fize, Matthieu Koepf, Phong D. Tran, Murielle Chavarot-Kerlidou, Vincent Artero

UNASSISTED SOLAR SYNGAS PRODUCTION BY A MOLECULAR DYE-COBALT CATALYST ASSEMBLY IN A TANDEM PHOTOELECTROCHEMICAL CELL

Duc N. Nguyen,[§,a,b] Emmanouil Giannoudis,[§,a] Tatiana Straistari,[a] Jennifer Fize,[a] Matthieu Koepf,[a] Phong D. Tran,[b,] Murielle Chavarot-Kerlidou,[a,*] Vincent Artero.[a,*]*

a. Univ. Grenoble Alpes, CNRS, CEA, IRIG, Laboratoire de Chimie et Biologie des Métaux, 17 rue des Martyrs, F-38054 Grenoble, France.

b. University of Science and Technology of Hanoi, Vietnam Academy of Science and Technology, 18 Hoang Quoc Viet, Hanoi, 100000 Vietnam.

Corresponding Authors

*Phong D. Tran, Email: tran-dinh.phong@usth.edu.vn; Murielle Chavarot-Kerlidou, Email: murielle.chavarot-kerlidou@cea.fr. Vincent Artero, Email: vincent.artero@cea.fr.

ABSTRACT. The ecological transition requires the development of carbon capture and utilization technologies powered with renewable energies. Direct solar conversion of CO_2 in photoelectrochemical cells is a promising approach to produce syngas, en route to fuels and chemicals. We report here on a dyad based on a Ru-based metallorganic dye and a tetraazamacrocyclic cobalt catalyst grafted on NiO to form efficient molecular photocathodes for CO-rich syngas production (ratio CO/H_2 > 80:20) from a CO_2-saturated aqueous bicarbonate buffer. After integration with a $BiVO_4$/CoPi photoanode in a tandem photoelectrochemical cell in a Z-scheme configuration, syngas could be produced from CO_2 water with Faradaic efficiencies of 62% and 14% for CO and H_2, respectively under visible light and in the absence of any applied bias, equating to a solar to fuel conversion efficiency of 1.3 10^{-2} %.

TOC GRAPHICS

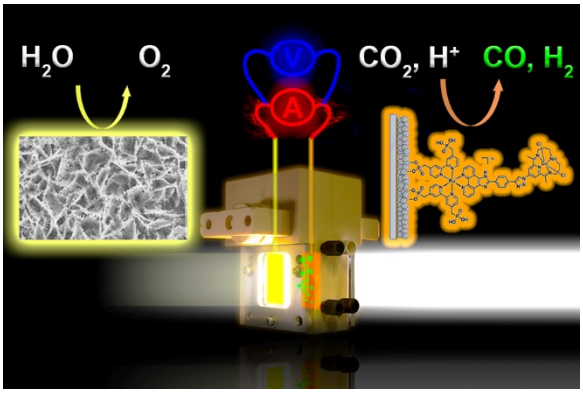

Beyond achieving a global reduction of carbon dioxide (CO_2) emissions, transforming this greenhouse gas into valuable chemical feedstocks is one major challenge to meet the 2015 Paris agreement target and contribute to mitigate climate change. Production of carbon-based fuels and commodity chemicals from CO_2 indeed represents a unique way to move away from the use of fossil resources and establish a circular carbon economy.[1] In Nature, conversion of CO_2 into carbohydrates – chemical fuels for living organisms – is achieved using sunlight as sole energy source, thanks to a complex photosynthetic machinery integrating key components for light harvesting and multielectronic redox catalysis.[2] This fascinating process provides guidelines to develop artificial photosynthetic devices for the direct sunlight-to-fuels conversion, with CO_2 conversion in photoelectrochemical cells (PECs) being one attractive approach.[3-4] One class of such integrated devices assemble two photoelectrodes in a tandem configuration replicating the Z-scheme of natural photosynthesis.[5] To implement them more easily, each photoelectrode is developed and optimized independently, *i.e*. under a three-electrode setup configuration. There are, however, several constraints on the selection of an effective combination of photoelectrodes to perform the reaction of interest under unassisted (electrical bias-free) conditions; the most critical one is certainly that they should both operate at the same current and at the same potential under irradiation, also in the same electrolyte conditions (nature, pH…). Great achievements were made over the last years with photoanode materials such as $BiVO_4$ driving photoelectrochemical water oxidation at onset potentials as low as +0.2V vs RHE, *i.e*. ~1V below the thermodynamic potential of 1.23V vs RHE.[6-7] With a bandgap of 2.4 eV, $BiVO_4$ can indeed absorb a large portion of visible light and it is stable in aqueous solution at pH values close to neutrality. On the photocathode side, however, reducing CO_2 with sunlight at such positive potentials is highly challenging. In this respect, a dye-sensitized approach offers greater flexibility than low band-gap

inorganic semiconductors to design photocathodes active over a wide range of potentials[8-18] and a few proof of concept examples for *unassisted* CO_2 reduction in tandem dye-sensitized photoelectrochemical cells (DS-PECs) were recently made with photocathodes assembling molecular rhenium[10] or ruthenium[15-16] catalysts with a ruthenium tris-diimine light-harvesting unit.

On the other hand, molecular cobalt complexes are attractive catalysts for solar fuels production.[19-20] Photoelectrochemical CO_2 reduction was achieved with *p*-type silicon photocathodes functionalized with a cobalt bis-terpyridine catalyst; yet, mixed organic/aqueous electrolytes are required for catalysis to be selective over proton reduction.[21-22] In contrast, a cobalt quaterpyridine catalyst anchored onto a *p*-type $Cu(In,Ga)Se_2$ (CIGS) semiconductor electrode proved to be highly active and selective for CO production in fully aqueous medium.[23] In both cases (*p*-Si and CIGS) however, the onset potentials at which photocurrents are generated are not positive enough to allow efficient coupling with a water oxidation photoanode under bias-free conditions. Cobalt phthalocyanine catalysts were also successfully employed,[24-25] and are the basis of the sole example of *unassisted* photoelectrochemical CO_2 reduction driven by molecular cobalt catalyst, reported by the group of E. Reisner with a wireless device (artificial leaf).[26] In this context, expanding and diversifying the range of effective molecular cobalt catalysts appears to be a promising strategy for designing efficient photoelectrochemical devices. This motivated us to investigate the light-driven CO_2 reduction activity of the tetraazamacrocyclic complex $[Co(N_4H)Cl_2]^+$ (**CoN_4H**),[27-28] the electrocatalytic activity for CO_2 reduction of which was recently reexamined by the group of McCrory.[29] Following the approach we have previously developed for photoelectrochemical hydrogen production,[30-32] we report here the first synthesis of a covalent dye-catalyst assembly **RuP_4-CoN_4H** together with the aqueous photoelectrochemical activity of the corresponding NiO-based photocathode (Figure 1) in a three-electrode configuration. The

demonstration of photocurrents reaching −100 μA.cm^{-2} at +0.2V vs RHE allowed to successfully assemble this photocathode with a $BiVO_4$/CoPi photoanode, for syngas production from water and CO_2 in a functional tandem DS-PEC under bias-free conditions.

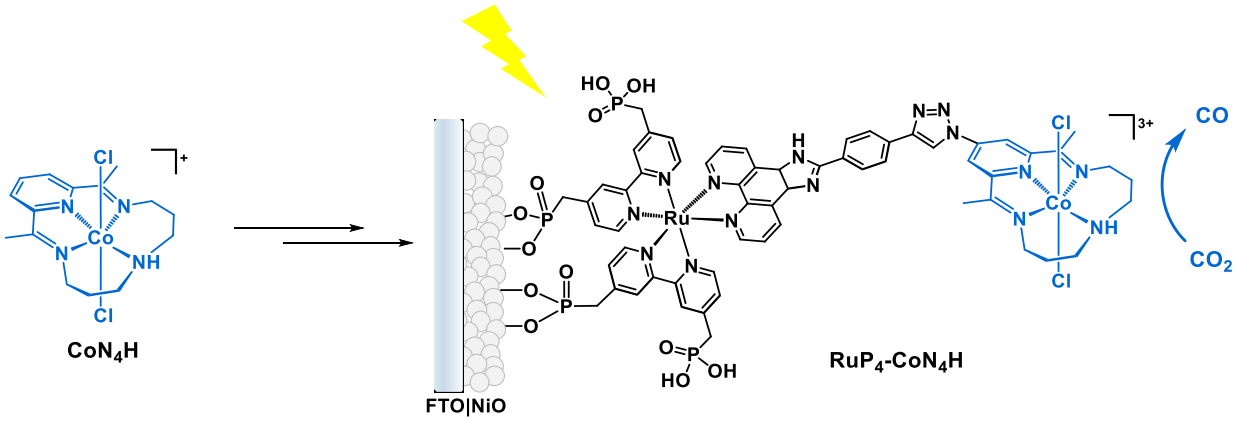

Figure 1. Structure of **CoN_4H** and schematic representation of the NiO-based photocathode based on the molecular dyad **RuP_4-CoN_4H**.

Photocathode preparation and characterization. The dyad **RuP_4^{OEt}-CoN_4H** was synthesized by a stepwise procedure based on a copper-catalyzed azide-alkyne cycloaddition (CuAAC) coupling between the alkyne-substituted **RuP_4^{OEt}-EPIP**[33] complex and the 4-azido-2,6-diacetylpyridine precursor, followed by the template synthesis of the tetraazamacrocyclic cobalt catalyst **CoN_4H**[32] (full synthetic details in SI, Schemes S1-2, Figures S1-2). The **RuP_4^{OEt}-CoN_4** dyad was spectroscopically (Figure S3) and electrochemically (Figure S4) characterized in solution prior to the hydrolysis of the phosphonate anchoring groups and the sensitization of homemade mesoporous NiO films.

Photoelectrochemical activity of the dye-sensitized NiO photocathode was first assessed under a three-electrode configuration setup in a CO_2-saturated aqueous $NaHCO_3$ solution (50 mM, pH 6.6) as electrolyte.[9] Linear sweep voltammograms (LSV) were recorded from +1.2 V to −0.2 V vs. RHE under chopped-light IR-filtered AM 1.5 G irradiation (Figure 2). Under irradiation, the **RuP_4-CoN_4H**-sensitized NiO films start exhibiting cathodic photocurrents at ~ +1.0 V vs. RHE,

ie 1.1 V more positive than the thermodynamic potential. Remarkably, the photocurrent density exceeds −100 μA.cm^{-2} (dark current substracted) at potentials more negative than +0.2 V vs. RHE (Figure 2). Both the onset potential and photocurrent density values are significantly higher than the ones previously reported for related dye-sensitized photocathodes active in aqueous media, which range from a few μA.cm^{-2} to a few tens of μA.cm^{-2} at much more negative applied potentials.[8-10, 13-16]

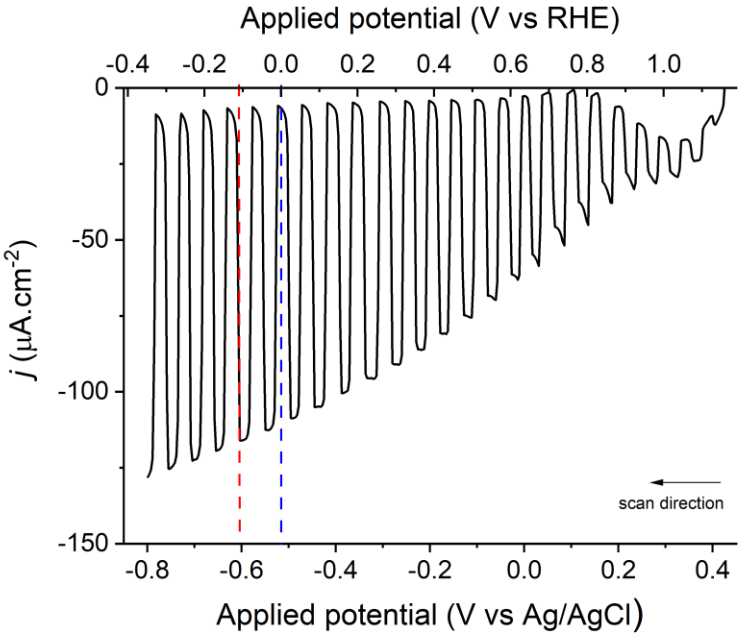

Figure 2. Linear sweep voltammogram of a NiO electrode sensitized by **RuP$_4$-CoN$_4$H** in a CO_2-saturated 50 mM $NaHCO_3$ aqueous solution at pH 6.6 under chopped light AM 1.5 G solar irradiation (IR filtered). The blue and red dashed lines indicate the equilibrium potentials for H^+/H_2 (0 V vs RHE) and CO_2/CO (−0.11 V vs RHE), respectively.

To confirm the origin of the observed photocurrents, three hours chronoamperometric experiments were conducted under continuous light irradiation at an applied potential of +0.19 V vs. RHE (−0.40V vs Ag/AgCl) in a CO_2-saturated electrolyte;[34] the compounds formed in the headspace (CO, H_2) and in the electrolyte (HCOOH) were quantified at the end of the run (Tables 1 & S1). Under these fully aqueous electrolyte conditions, the process is remarkably highly selective toward CO_2 reduction, with CO being the main carbon-based product formed (47 ± 7 %

F.E.$_{CO}$; 9 ± 2 % F.E.$_{H2}$; ratio CO/H_2 > 80:20) and a turnover number (TON_{CO}) of 110 according to the Co loading of 2.8 nmol.cm^{-2} determined by ICP-AES. In contrast, when a N_2-saturated aqueous electrolyte was used, similar photocurrents and charge densities were recorded (Figure S6), but H_2 is the main product (Tables 1 & S1) with only traces of CO detected (< 5% F.E.), likely originated from CO_2 released from the bicarbonate buffer. Control experiments using either pristine or **RuP$_4$-DAP**-sensitized NiO films displayed significantly lower photocurrents compared to the **RuP$_4$-CoN$_4$H** photocathode (Figure S5); moreover, only traces of CO were detected in the absence of the **CoN$_4$H** catalyst at the surface of the film (Table 1). These results clearly support a cobalt-based mechanism for the observed activity. Of note, low to significant amounts of HCOOH were also produced, including in control experiments performed with pristine NiO electrode or in the absence of added CO_2. This indicates that formate is not produced via a mechanism involving the **CoN$_4$H** catalyst but rather thanks to Ni-based active sites generated at the NiO surface.

Table 1. Photoelectrochemical performances of the different photocathode assemblies (selected examples; see Table S1 for full set of data). Chronoamperomeric measurements were recorded under continuous irradiation (IR-filtered simulated AM 1.5 G solar irradiation) for 3 hours in a CO_2-saturated aqueous $NaHCO_3$ electrolyte (pH = 6.6) at an applied potential of +0.19 V vs RHE (−0.4 V vs Ag/AgCl). Amounts of CO (n_{CO}), H_2 (n_{H2}) and HCOOH (n_{HCOOH}) produced are given in nmol.cm^{-2}.

Photocathode	**Charge** (mC.cm^{-2})	**n_{CO}** (FE_{CO})	**n_{H2}** (FE_{H2})	**n_{HCOOH}** (FE_{HCOOH})	**CO/H_2 ratio**
NiO	11	1 (2%)	1 (2%)	23 (38%)	—
NiO|**RuP$_4$-DAP**	32	2 (1%)	8 (5%)	33 (20%)	—
NiO|**RuP$_4$-CoN$_4$H**	143	307 (42%)	61 (8%)	60 (8%)	83:17
NiO|**RuP$_4$-CoN$_4$H** (no CO_2)[a]	98	15 (3%)	154 (31%)	50 (10%)	9:91

a- N_2-purged electrolyte.

Of note, although a high photocurrent is recorded at the beginning of the three-hour chronoamperometric measurement, a fast decrease is observed over time (Figure S5). In addition,

post-operando quantification by ICP-AES of the Co present at the surface of the electrode revealed a significant percentage of loss during the course of the experiment (85 % for two independent experiments). Phosphonate grafting is reported to be stable in aqueous solutions below pH 5 whereas optimized conditions for photoelectrochemical CO_2 reduction require to work in near-neutral electrolytes. The loss of activity is therefore very likely due to the release of the dyad in the electrolyte solution, as previously observed for related phosphonate-based dye-sensitized photocathodes.[10, 31] Strategies reported to effectively increase the stability of the phosphonate anchoring, typically by ALD deposition of a thin layer of oxide[35] or by embedding the molecular components in a polymer matrix,[16] will have to be implemented in the future to prevent the deactivation of the photocathode.

Photoelectrochemical activity in a tandem cell configuration. The photoelectrochemical performances of NiO|**RuP_4-CoN_4H**, with notable photocurrents recorded at high positive onset potential under near-neutral pH electrolyte conditions, makes this photocathode an excellent candidate to be assessed in a tandem cell configuration, in the absence of any additional electrical bias. We selected a $BiVO_4$|CoPi photoanode able to achieve water oxidation and deliver the electrons and protons consumed at the photocathode to reduce CO_2. $BiVO_4$ photoanodes were prepared via electrodeposition of BiOI onto a FTO glass substrate, followed by introduction of the [$VO(acac)_2$] (acacH = acetylacetone) vanadium precursor and thermal annealing according to the procedure previously reported by Le *et al.*[36] A layer of CoPi water-oxidation cocatalyst was deposited onto the ~900 nm thick $BiVO_4$ film, using an electrodeposition procedure adapted from Nocera *et coll.*[37]

The photoelectrodes were introduced into a custom-made photoelectrochemical cell (Figure S7) in a true tandem configuration (Figure 3a). We tested various configurations regarding the choice

of the photoelectrode to be placed first in the optical path and the direction of illumination. We kept a configuration where the two photoelectrodes are facing each other in order to optimize ion migration. Best results were obtained when the NiO|**RuP_4-CoN_4H** photocathode was placed in front of the $BiVO_4$|CoPi photoanode. In this configuration, the photocathode is back-illuminated while the photoanode is front-illuminated. A Nafion® proton exchange membrane was fitted at the middle point of the space between the photoelectrodes to equally divide the working volume into two compartments. With both photoelectrodes in place, linear sweep voltammograms were independently recorded for the photoanode and the photocathode in a three-electrode configuration setup, in an aqueous $NaHCO_3$ solution (50 mM, pH 6.6) as electrolyte and under simulated solar irradiation. Under these conditions, cathodic photocurrents are generated from +0.80 V *vs* RHE at the photocathode; on the other hand, anodic photocurrents are generated from +0.35 V vs RHE at the photoanode shaded by the photocathode (Figure S8). The plot of the absolute current densities obtained with photoelectrodes of 3.0 cm^2, versus the applied potential (Figure 3b) shows more clearly that both electrodes are active on a same range of potentials, which is a prerequisite for testing them together in a tandem configuration; from the intersection of the curves, an operating photocurrent of 123 µA is predicted to be generated at an operating potential of +0.44V *vs.* RHE in a two-electrode configuration setup.

a)

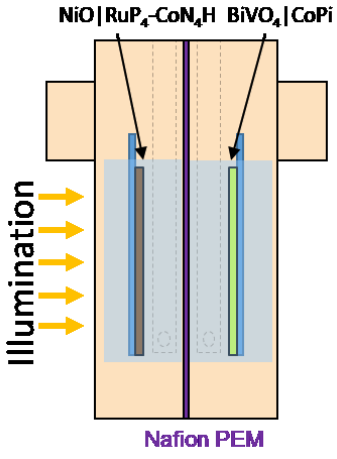

b)

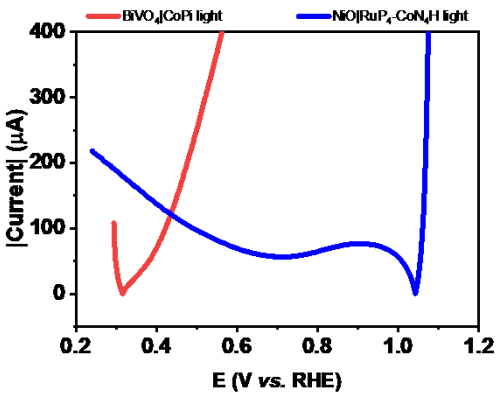

c)

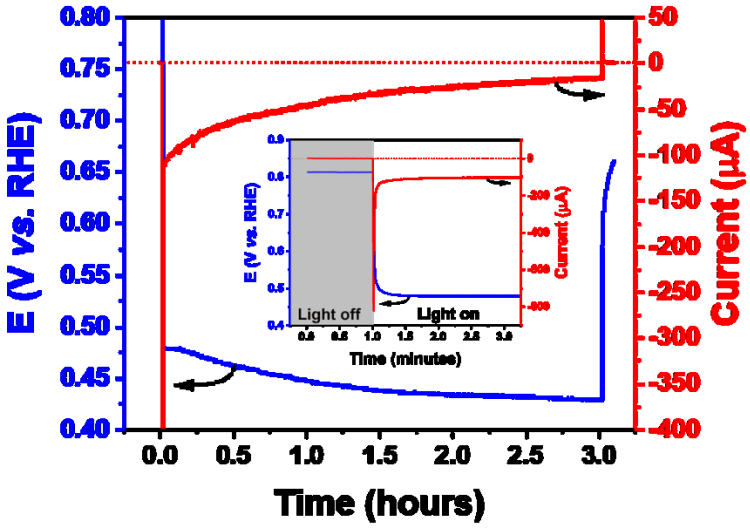

Figure 3. (a) Schematic representation of the photoelectrodes in the tandem photoelectrochemical cell. (b) Linear sweep voltammograms (absolute current values obtained from 3.0 cm^2 photoelectrodes) of the NiO|**RuP_4-CoN_4H** photocathode (blue line) and of the $BiVO_4$|CoPi photoanode (red line) recorded under light irradiation conditions shaded by the photocathode and the membrane; the intersection between the red and blue photocurrent curves corresponds to the expected operation potential under a tandem cell configuration. (c) 3 hours chronoamperometric and chronopotentiometric measurements recorded in the tandem cell configuration (the potential was measured at the cathode). Conditions: CO_2-saturated aqueous 50 mM $NaHCO_3$ at pH 6.6 under AM 1.5G light irradiation, scan rate 10 $mV.s^{-1}$. See Figure S9 for details about the monitoring of the performances.

The photoelectrochemical activity in the tandem cell configuration was then measured with a bipotentiostat setup where both the current running through the system and the potential of the photocathode (short-circuited with the photoanode) were simultaneously recorded (a detailed description can be found in Figure S9). Of note in this configuration, the current was measured with the photocathode set at 0 V vs the potential of the photoanode used as both reference and counter electrode so that no additional electrical bias was applied to the system.[38] When switching on the light, an initial photocurrent of 111 µA is generated at a recorded operating potential of +0.48V *vs.* RHE (Figure 3c). These two values are very close to the ones predicted from the individual characterization of both photoelectrodes, confirming the viability of the bipotentiostat setup employed here as a direct method to continuously monitor the performances of the system

working in a true tandem cell configuration. The photocurrent decreases steadily over time, reaching 65 µA for an operating potential of +0.46 V vs RHE after 30 min, and 30 µA for an operating potential of +0.43 V vs RHE after three hours. This decay in performances parallels the evolution of the photocathode performances over time, as described above. At the end of the three-hour experiment, 1381 nmol CO and 319 nmol H_2 were produced with Faradaic efficiencies of 62% and 14%, respectively (CO/H_2 ratio of 82:18; see Table S2 and Figure S10 for triplicate measurements); the high selectivity of NiO|**RuP$_4$-CoN$_4$H** for CO_2 over proton reduction is thus fully preserved in the tandem cell setup operating at +0.48V *vs.* RHE. This production of CO and H_2 corresponds to an overall solar-to-fuel conversion efficiency (η_{STF}) of 1.3 10^{-2} % (see SI for details), thus close to the highest values of 1.7 10^{-2} % and 4.8 10^{-2} %, so far reported for two unbiased tandem DS-PECs assembling a $BiVO_4$/CoOx photoanode with NiO|pRu-*poly*-Ru-Ru_{cat} photocathodes integrating the ruthenium-based $Ru(bpy)(CO)_2Cl_2$ catalyst.[15-16] Of note, in this study, electropolymerization of the Ru dye molecules at the surface of the NiO film drastically increased the stability and therefore the performances of the device.

Pursuing the research efforts on the integration of molecular CO_2 reduction catalysts in photoelectrochemical devices is essential to eventually contribute to the development of atom-saving, cost-effective and sustainable energy conversion processes. In this study, photoelectrochemical CO_2 reduction was demonstrated for the first time with a dye-sensitized photocathode based on a molecular cobalt catalyst, the tetraazamacrocyclic complex **CoN$_4$H**. Remarkable performances were achieved for the production of CO_2-neutral syngas in fully aqueous electrolyte, with photocurrent densities among the highest so far reported for molecular-based photocathodes and a high positive onset potential (+1V vs RHE) for photoelectrochemical

activity. The latter feature was instrumental to couple this photocathode with a $BiVO_4$-based photoanode for water oxidation in a tandem photoelectrochemical cell functional under non-biased conditions. This paves the way towards the use of dyes exclusively made of earth-abundant elements as well as surface engineering strategies to optimize the molecular loading in order to further increase the performances.

ASSOCIATED CONTENT

Supporting Information. The following files are available free of charge. Detailed synthetic procedures, additional spectroscopic and photoelectrochemical data and schematic description of the tandem cell (PDF).

AUTHOR INFORMATION

§ These authors contributed equally to the work.

@Solhycat

www.solhycat.com

Notes

The authors declare no competing financial interest.

ACKNOWLEDGMENT

This work was supported by the French National Research Agency (Labex ARCANE, CBH-EUR-GS, ANR-17-EURE-0003; PhotoCarb project, ANR-16-CE05-0025-03). EG acknowledges CEA for funding through a CFR PhD grant. Duc N. Nguyen and Phong D. Tran acknowledge National

Foundation for Science and Technology Development through the research grant NAFOSTED 103.99-2019.328. Duc N. Nguyen thanks the French Embassy in Hanoi for an excellence grant.

REFERENCES

1. Segev, G.; Kibsgaard, J.; Hahn, C.; Xu, Z. J.; Cheng, W.-H.; Deutsch, T. G.; Xiang, C.; Zhang, J. Z.; Hammarström, L.; Nocera, D. G.; Weber, A. Z.; Agbo, P.; Hisatomi, T.; Osterloh, F. E.; Domen, K.; Abdi, F. F.; Haussener, S.; Miller, D. J.; Ardo, S.; McIntyre, P. C.; Hannappel, T.; Hu, S.; Atwater, H.; Gregoire, J. M.; Ertem, M. Z.; Sharp, I. D.; Choi, K.-S.; Lee, J. S.; Ishitani, O.; Ager, J. W.; Prabhakar, R. R.; Bell, A. T.; Boettcher, S. W.; Vincent, K.; Takanabe, K.; Artero, V.; Napier, R.; Cuenya, B. R.; Koper, M. T. M.; Van De Krol, R.; Houle, F., The 2022 solar fuels roadmap. *J. Phys. D: Appl. Phys.* **2022,** *55* (32), 323003.
2. Barber, J., Photosynthetic energy conversion: natural and artificial. *Chem. Soc. Rev.* **2009,** *38* (1), 185-196.
3. Kumaravel, V.; Bartlett, J.; Pillai, S. C., Photoelectrochemical Conversion of Carbon Dioxide (CO_2) into Fuels and Value-Added Products. *ACS Energy Lett.* **2020,** *5* (2), 486-519.
4. Reyes Cruz, E. A.; Nishiori, D.; Wadsworth, B. L.; Nguyen, N. P.; Hensleigh, L. K.; Khusnutdinova, D.; Beiler, A. M.; Moore, G. F., Molecular-Modified Photocathodes for Applications in Artificial Photosynthesis and Solar-to-Fuel Technologies. *Chem. Rev.* **2022,** *122* (21), 16051-16109.
5. Kim, J. H.; Hansora, D.; Sharma, P.; Jang, J.-W.; Lee, J. S., Toward practical solar hydrogen production – an artificial photosynthetic leaf-to-farm challenge. *Chem. Soc. Rev.* **2019,** *48* (7), 1908-1971.
6. Kim, T. W.; Choi, K.-S., Nanoporous $BiVO_4$ Photoanodes with Dual-Layer Oxygen Evolution Catalysts for Solar Water Splitting. *Science* **2014,** *343* (6174), 990-994.
7. Ding, C.; Shi, J.; Wang, D.; Wang, Z.; Wang, N.; Liu, G.; Xiong, F.; Li, C., Visible light driven overall water splitting using cocatalyst/$BiVO_4$ photoanode with minimized bias. *Phys. Chem. Chem. Phys.* **2013,** *15* (13), 4589-4595.
8. Sahara, G.; Abe, R.; Higashi, M.; Morikawa, T.; Maeda, K.; Ueda, Y.; Ishitani, O., Photoelectrochemical CO_2 reduction using a Ru(II)-Re(I) multinuclear metal complex on a p-type semiconducting NiO electrode. *Chem. Commun.* **2015,** *51* (53), 10722-10725.
9. Sahara, G.; Kumagai, H.; Maeda, K.; Kaeffer, N.; Artero, V.; Higashi, M.; Abe, R.; Ishitani, O., Photoelectrochemical Reduction of CO_2 Coupled to Water Oxidation Using a Photocathode with a Ru(II)–Re(I) Complex Photocatalyst and a CoOx/TaON Photoanode. *J. Am. Chem. Soc.* **2016,** *138* (42), 14152-14158.
10. Kumagai, H.; Sahara, G.; Maeda, K.; Higashi, M.; Abe, R.; Ishitani, O., Hybrid photocathode consisting of a $CuGaO_2$ p-type semiconductor and a Ru(II)–Re(I) supramolecular photocatalyst: non-biased visible-light-driven CO_2 reduction with water oxidation. *Chem. Sci.* **2017,** *8* (6), 4242-4249.
11. Wang, D.; Wang, Y.; Brady, M. D.; Sheridan, Matthew V.; Sherman, B. D.; Farnum, B. H.; Liu, Y.; Marquard, S. L.; Meyer, G. J.; Dares, C. J.; Meyer, T. J., A donor-chromophore-catalyst assembly for solar CO_2 reduction. *Chem. Sci.* **2019,** *10* (16), 4436-4444.

12. Li, T.-T.; Shan, B.; Meyer, T. J., Stable Molecular Photocathode for Solar-Driven CO_2 Reduction in Aqueous Solutions. *ACS Energy Lett.* **2019,** *4* (3), 629-636.
13. Kamata, R.; Kumagai, H.; Yamazaki, Y.; Sahara, G.; Ishitani, O., Photoelectrochemical CO_2 Reduction Using a Ru(II)–Re(I) Supramolecular Photocatalyst Connected to a Vinyl Polymer on a NiO Electrode. *ACS Appl. Mater. Interfaces* **2019,** *11* (6), 5632-5641.
14. Cerpentier, F. J. R.; Karlsson, J.; Lalrempuia, R.; Brandon, M. P.; Sazanovich, I. V.; Greetham, G. M.; Gibson, E. A.; Pryce, M. T., Ruthenium Assemblies for CO_2 Reduction and H_2 Generation: Time Resolved Infrared Spectroscopy, Spectroelectrochemistry and a Photocatalysis Study in Solution and on NiO. *Frontiers in Chemistry* **2021,** *9*, 795877.
15. Kuttassery, F.; Kumagai, H.; Kamata, R.; Ebato, Y.; Higashi, M.; Suzuki, H.; Abe, R.; Ishitani, O., Supramolecular photocatalysts fixed on the inside of the polypyrrole layer in dye sensitized molecular photocathodes: application to photocatalytic CO_2 reduction coupled with water oxidation. *Chem. Sci.* **2021,** *12* (39), 13216-13232.
16. Kamata, R.; Kumagai, H.; Yamazaki, Y.; Higashi, M.; Abe, R.; Ishitani, O., Durable photoelectrochemical CO_2 reduction with water oxidation using a visible-light driven molecular photocathode. *J. Mater. Chem. A* **2021,** *9* (3), 1517-1529.
17. Shan, B.; Vanka, S.; Li, T.-T.; Troian-Gautier, L.; Brennaman, M. K.; Mi, Z.; Meyer, T. J., Binary molecular-semiconductor p–n junctions for photoelectrocatalytic CO_2 reduction. *Nat. Energy* **2019,** *4* (4), 290-299.
18. Miró, R.; Guzmán, H.; Godard, C.; Gual, A.; Zammillo, F.; Schubert, T. J. S.; Iliev, B.; Chiodoni, A.; Hernández, S.; de los Bernardos, M. D., Solar-driven CO_2 reduction catalysed by hybrid supramolecular photocathodes and enhanced by ionic liquids. *Catal. Sci. Technol.* **2023,** *13* (6), 1708-1717.
19. Artero, V.; Chavarot-Kerlidou, M.; Fontecave, M., Splitting water with cobalt. *Angew. Chem. Int. Ed.* **2011,** *50*, 7238-7266.
20. Dalle, K. E.; Warnan, J.; Leung, J. J.; Reuillard, B.; Karmel, I. S.; Reisner, E., Electro- and Solar-Driven Fuel Synthesis with First Row Transition Metal Complexes. *Chem. Rev.* **2019,** *119* (4), 2752-2875.
21. Leung, J. J.; Warnan, J.; Ly, K. H.; Heidary, N.; Nam, D. H.; Kuehnel, M. F.; Reisner, E., Solar-driven reduction of aqueous CO_2 with a cobalt bis(terpyridine)-based photocathode. *Nat. Catal.* **2019,** *2* (4), 354-365.
22. Leung, J. J.; Vigil, J. A.; Warnan, J.; Edwardes Moore, E.; Reisner, E., Rational Design of Polymers for Selective CO_2 Reduction Catalysis. *Angew. Chem. Int. Ed.* **2019,** *58* (23), 7697-7701.
23. Pati, P. B.; Wang, R.; Boutin, E.; Diring, S.; Jobic, S.; Barreau, N.; Odobel, F.; Robert, M., Photocathode functionalized with a molecular cobalt catalyst for selective carbon dioxide reduction in water. *Nat. Commun.* **2020,** *11* (1), 3499.
24. Roy, S.; Miller, M.; Warnan, J.; Leung, J. J.; Sahm, C. D.; Reisner, E., Electrocatalytic and Solar-Driven Reduction of Aqueous CO_2 with Molecular Cobalt Phthalocyanine–Metal Oxide Hybrid Materials. *ACS Catal.* **2021,** *11* (3), 1868-1876.
25. Shang, B.; Rooney, C. L.; Gallagher, D. J.; Wang, B. T.; Krayev, A.; Shema, H.; Leitner, O.; Harmon, N. J.; Xiao, L.; Sheehan, C.; Bottum, S. R.; Gross, E.; Cahoon, J. F.; Mallouk, T. E.; Wang, H., Aqueous Photoelectrochemical CO_2 Reduction to CO and Methanol over a Silicon Photocathode Functionalized with a Cobalt Phthalocyanine Molecular Catalyst. *Angew. Chem. Int. Ed.* **2023,** *62* (4), e202215213.
26. Andrei, V.; Reuillard, B.; Reisner, E., Bias-free solar syngas production by integrating a molecular cobalt catalyst with perovskite–$BiVO_4$ tandems. *Nat. Mater.* **2020,** *19* (2), 189-194.

27. Lacy, D. C.; McCrory, C. C. L.; Peters, J. C., Studies of Cobalt-Mediated Electrocatalytic CO_2 Reduction Using a Redox-Active Ligand. *Inorg. Chem.* **2014,** *53* (10), 4980-4988.
28. Tinnemans, A. H. A.; Koster, T. P. M.; Thewissen, D. H. M. W.; Mackor, A., Tetraaza-macrocyclic cobalt(II) and nickel(II) complexes as electron-transfer agents in the photo(electro)chemical and electrochemical reduction of carbon dioxide. *Recl. Trav.Chim. Pays-Bas* **1984,** *103* (10), 288-295.
29. Nie, W.; Tarnopol, D. E.; McCrory, C. C. L., Enhancing a Molecular Electrocatalyst's Activity for CO_2 Reduction by Simultaneously Modulating Three Substituent Effects. *J. Am. Chem. Soc.* **2021,** *143* (10), 3764-3778.
30. Kaeffer, N.; Massin, J.; Lebrun, C.; Renault, O.; Chavarot-Kerlidou, M.; Artero, V., Covalent Design for Dye-Sensitized H_2-Evolving Photocathodes Based on a Cobalt Diimine–Dioxime Catalyst. *J. Am. Chem. Soc.* **2016,** *138* (38), 12308-12311.
31. Giannoudis, E.; Bold, S.; Müller, C.; Schwab, A.; Bruhnke, J.; Queyriaux, N.; Gablin, C.; Leonard, D.; Saint-Pierre, C.; Gasparutto, D.; Aldakov, D.; Kupfer, S.; Artero, V.; Dietzek, B.; Chavarot-Kerlidou, M., Hydrogen Production at a NiO Photocathode Based on a Ruthenium Dye–Cobalt Diimine Dioxime Catalyst Assembly: Insights from Advanced Spectroscopy and Post-operando Characterization. *ACS Appl. Mater. Interfaces* **2021,** *13* (42), 49802-49815.
32. Bold, S.; Massin, J.; Giannoudis, E.; Koepf, M.; Artero, V.; Dietzek, B.; Chavarot-Kerlidou, M., Spectroscopic Investigations Provide a Rationale for the Hydrogen-Evolving Activity of Dye-Sensitized Photocathodes Based on a Cobalt Tetraazamacrocyclic Catalyst. *ACS Catal.* **2021,** *11* (6), 3662-3678.
33. Queyriaux, N.; Giannoudis, E.; Lefebvre, J.-F.; Artero, V.; Chavarot-Kerlidou, M., Synthesis of Ruthenium Tris-Diimine Photosensitizers Substituted by Four Methylphosphonate Anchoring Groups for Dye-Sensitized Photoelectrochemical Cell Applications. *Eur. J. Inorg. Chem.* **2019,** *2019* (15), 2154-2161.
34. From data in Table 1, less than 1% of the CO_2 initially dissolved in the electrolyte is converted within the three-hour experiment, so that we can consider that the solution remains saturated throughout the measurement.
35. Wang, D.; Huang, Q.; Shi, W.; You, W.; Meyer, T. J., Application of Atomic Layer Deposition in Dye-Sensitized Photoelectrosynthesis Cells. *Trends in Chemistry* **2021,** *3* (1), 59-71.
36. Le, H. V.; Nguyen, M. D.; Pham, Y. T. H.; Nguyen, D. N.; Le, L. T.; Han, H.; Tran, P. D., Decoration of AgOx hole collector to boost photocatalytic water oxidation activity of $BiVO_4$ photoanode. *Mater. Today Energy* **2021,** *21*, 100762.
37. Lutterman, D. A.; Surendranath, Y.; Nocera, D. G., A Self-Healing Oxygen-Evolving Catalyst. *J. Am. Chem. Soc.* **2009,** *131* (11), 3838-3839.
38. Nguyen, D. N.; Fadel, M.; Chenevier, P.; Artero, V.; Tran, P. D., Water-Splitting Artificial Leaf Based on a Triple-Junction Silicon Solar Cell: One-Step Fabrication through Photoinduced Deposition of Catalysts and Electrochemical Operando Monitoring. *J. Am. Chem. Soc.* **2022,** *144* (22), 9651-9660.